Solvent-Dependent Cage Dynamics of Small Nonpolar Radicals: Lessons from the Photodissociation and Geminate Recombination of Alkylcobalamins

Andrew B. Stickrath, Elizabeth C. Carroll, Xiaochuan Dai, D. Ahmasi Harris, Aaron Rury, Broc Smith, Kuo-Chun Tang, Jonathan Wert, and Roseanne J. Sension*

Department of Chemistry, Department of Physics, and Program in Applied Physics, University of Michigan, 930 North University Avenue, Ann Arbor, Michigan 48109-1055

Received: February 26, 2009; Revised Manuscript Received: May 30, 2009

Time-resolved transient absorption spectroscopy was used to investigate the primary geminate recombination and cage escape of alkyl radicals in solution over a temperature range from 0 to 80 °C. Radical pairs were produced by photoexcitation of methyl, ethyl, propyl, hexylnitrile, and adenosylcobalamin in water, ethylene glycol, mixtures of water and ethylene glycol, and sucrose solutions. In contrast to previous studies of cage escape and geminate recombination, these experiments demonstrate that cage escape for these radical pairs occurs on time scales ranging from a hundred picoseconds to over a nanosecond as a function of solvent fluidity and radical size. Ultrafast cage escape (<100 ps) is only observed for the methyl radical where the radical pair is produced through excitation to a directly dissociative electronic state. The data are interpreted using a unimolecular model with competition between geminate recombination and cage escape. The escape rate constant, k_e, is not a simple function of the solvent fluidity (T/η) but depends on the nature of the solvent as well. The slope of k_e as a function of T/η for the adenosyl radical in water is in near quantitative agreement with the slope calculated using a hydrodynamic model and the Stokes−Einstein equation for the diffusion coefficients. The solvent dependence is reproduced when diffusion constants are calculated taking into account the relative volume and mass of both solvent and solute using the expression proposed by Akgerman (Akgerman, A.; Gainer, J. L. *Ind. Eng. Chem. Fundam.* **1972**, *11*, 373−379). Rate constants for cage escape of the other radicals investigated are consistently smaller than the calculated values suggesting a systematic correction for radical size or coupled radical pair motion.

I. Introduction

The influence of local environment on the geminate recombination and cage escape of reactive species in solution is a topic of great significance for detailed modeling of chemical reactivity. This question has excited the interest of many researchers, both experimentalists and theorists, for 70 years or more. Yet the problem is not solved. A qualitative understanding is straightforward. Diffusive cage escape and recombination of radical pairs is expected to depend linearly on the sum of the diffusion constants of the radicals. For diffusion of the radical pair in a continuum solvent the self-diffusion coefficient can be approximated by using the Stokes−Einstein expression

$$D = \frac{k_b T}{6\pi r \eta} \tag{1}$$

where k_b is the Boltzmann constant, r is the radius of the radical (assumed to be spherical), T is the temperature, and η is the shear viscosity of the solvent. The factor of 6π in the denominator assumes stick boundary conditions, while a factor of 4π is derived for slip boundary conditions. Thus cage escape and recombination are expected to depend linearly on the solvent fluidity (T/η) and inversely on the radical size or radius. Such qualitative trends are observed in the data, but quantitative agreement between theoretical prediction and experimental measurement remains elusive. One of the complications lies in development of experimentally accessible probes of the intrinsic dynamical processes. Early studies used steady-state spectroscopic methods to investigate the photoinitiated dissociation of iodine molecules.[1] This allowed direct comparison with theoretical predictions and models.[2,3] Steady-state spectroscopic methods have been applied to study geminate recombination in many other systems, including alkylcobalamins.[4,5]

The development of time-resolved spectroscopies with picosecond and femtosecond resolution allowed for much more direct measurement of diffusive cage escape and geminate recombination. Again the iodine molecule became a favored paradigm, with early studies investigating the dissociation, geminate recombination, and vibrational relaxation of iodine as a function of solvent.[6−19] Studies have also been performed to investigate geminate recombination following excitation of larger neutral radicals.[20−31] The measurements on these caged radical pairs produced by photodissociation again provide qualitative agreement with predicted trends, escape rates depend on radical size and solvent fluidity, but quantitative agreement is elusive.

Femtosecond and picosecond experimental measurements suggest that cage escape on time scales of a few picoseconds is common for all but the largest radicals.[29,32,33] Yet simple consideration of diffusive cage escape using the Stokes−Einstein formula for the diffusion coefficient suggests that cage escape should be a much slower process. Under stationary state conditions, when the lifetime of the radical pair is controlled by diffusive molecular movement, the rate constant for dissociation or cage escape, k_e, of a contact radical pair is[34]

* Corresponding author, rsension@umich.edu.

10.1021/jp9017986 CCC: $40.75
Published on Web 07/08/2009

$$k_e = \frac{D}{R^2} \quad (2)$$

where R is the contact radius or reactive radius of the radical pair and D is the sum of the self-diffusion coefficients of the two radicals. With eqs 1 and 2 the diffusion coefficient for a radical with a radius of 2 Å in a solvent of viscosity 1 mPa s at a temperature 298 K will be on the order of 1.1×10^{-5} cm^2/s and the rate constant for dissociation of the contact radical pair will be 1.4×10^{10} s^{-1}, or 0.014 ps^{-1}. That is cage escape should occur with an approximate time constant $\tau_e \approx 70$ ps. Measured rates of cage escape following photodissociation have been uniformly faster, often much faster than these simple estimates predict.

Some models for diffusive cage escape suggest a nonexponential decay of the geminate radical pair,[21,32−37] but the measured decays are still faster than the decays predicted by using reasonable parameters. Bultmann and Ernsting,[32] in their careful study of photodissociation, cage escape, and geminate recombination of bis(p-aminophenyl) disulfide find that the data suggest an unreasonable value for the diffusion coefficient, approximately 2 orders of magnitude larger than expected, and pursue other explanations for the observed data. The disagreement between quantitative estimates for dissociation of caged radicals and the available time-resolved data demonstrates that there is still a need for careful investigation of the cage dynamics and recombination of simple radicals in typical solvents.

In a recent series of papers we have explored the photodissociation and recombination of alkylcobalamins, especially the biologically active B_{12} coenzymes methylcobalamin (MeCbl) and 5′-deoxyadenosylcobalamin (AdoCbl), as a function of environment.[38−43] These studies were pursued to address questions of biochemical importance concerning the enzymatic generation and exploitation of free radicals. However, the photolysis of alkylcobalamins is interesting in its own right as a method for production of neutral radical pairs with well-defined initial conditions and a variety of sizes and properties. The spectral changes associated with changes in the ligation and oxidation state of the cobalt-containing corrin ring provides an excellent spectroscopic probe of the dissociation and geminate recombination. Thus the photolysis of alkylcobalamins provides a paradigm system to study the diffusive cage escape of small molecules in solution.

Excitation of an alkylcobalamin (Figure 1) with 400 nm light results in homolytic bond cleavage on a time scale of 100 ps or less with a quantum yield near unity for most alkyl ligands. The dynamics on time scales of 100 ps to 10 ns are then dominated by the competition between geminate recombination and diffusive separation of the radical pair. Thus the time scale for geminate recombination and cage escape is of the order expected for the diffusive cage escape of simple radicals. This is in direct contrast with most of the photodissociation studies reported in the literature.

In the studies reported here, we measure geminate recombination and cage escape for methyl, ethyl, *n*-propyl, *n*-hexylnitrile, and adenosyl radicals in a range of solvents and solvent mixtures over the temperature range between approximately 0 and 80 °C. These data provide the opportunity to investigate the diffusive behavior, including cage escape and geminate recombination of small radicals in solution in real time. The data agree well with hydrodynamic models for cage escape. These data also highlight the need to correct eq 1 to account for the influence of solvent, and solute mass and volume.

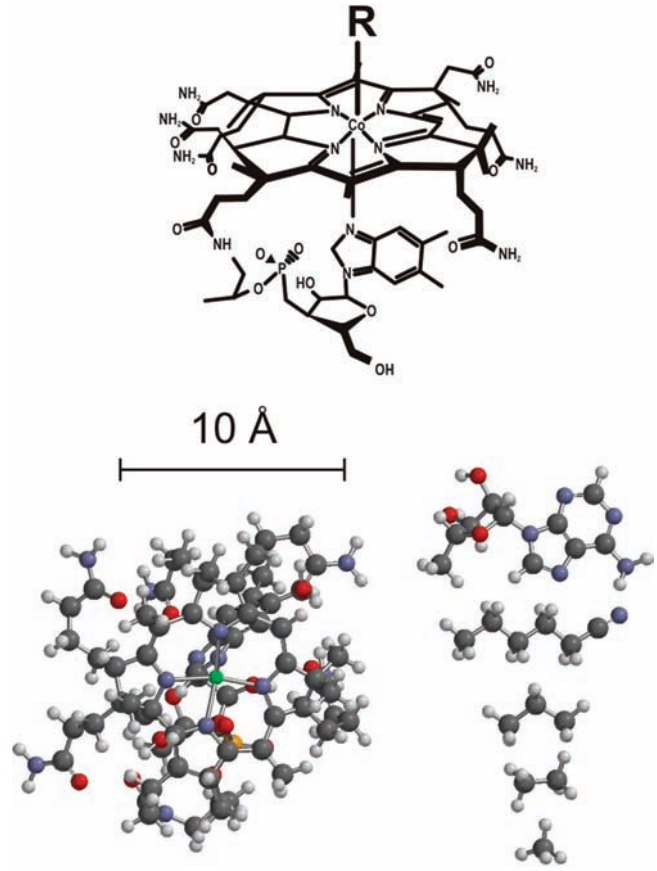

Figure 1. Top: Sketch of the alkylcobalamin structure observed in solution. The bottom axial ligand is supplied by a nitrogen from the appended dimethylbenzimidazole group. In the work described here the upper axial ligand is a methyl, ethyl, *n*-propyl, 5′-deoxyadenosyl, or *n*-hexylnitrile group. Bottom: Relative sizes of the cobalamin, adenosyl, hexylnitrile, propyl, ethyl, and methyl species. The models use the corresponding saturated species as approximations for the radicals.

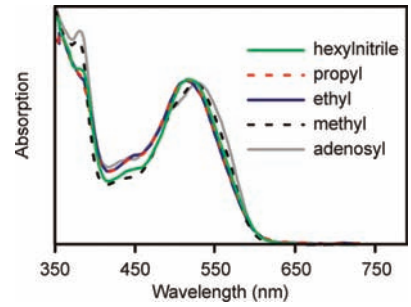

Figure 2. Absorption spectra of the alkylcobalamins used in these experiments. All of the species have the characteristic broad visible absorption at ca. 520 nm with a second strong absorption feature of comparable peak intensity beginning at 400 nm.

II. Experimental Section

Adenosylcobalamin and methylcobalamin were obtained from Sigma-Aldrich and used without further purification. Syntheses and purification of ethylcobalamin (EtCbl), *n*-propylcobalamin (PrCbl), and *n*-hexylnitrile cobalamin (HxnCbl) were carried out according to literature methods as described previously.[38] Cobalamin samples were prepared to a concentration of ca. 1 mM in aqueous solution, sucrose solution, ethylene glycol, or mixtures of ethylene glycol and water. The EtCbl and PrCbl solutions were somewhat less concentrated to conserve sample. The solutions were prepared, stored, and studied under anaerobic

conditions. Deoxygenated water was prepared by bubbling nitrogen gas through doubly distilled water for a minimum of 1 h before preparing the sample solutions. Ethylene glycol was deoxygenated using a freeze−pump−thaw cycle repeated three or four times before preparing the sample solutions. All cobalamin samples were maintained under a positive pressure atmosphere of nitrogen to exclude oxygen during the measurements. Temperature control was achieved by immersing the sample reservoir in a bath with a 50/50 mixture of water and ethylene glycol. The temperature of the bath was controlled by a Neslab RTE-111 refrigerated bath/circulator, capable of maintaining temperatures from −25 to +150 °C. The samples were flowed through a 1 mm path length cell to refresh the sample volume between laser pulses, and the temperature was measured with a temperature probe inserted in a T-joint located immediately after the sample cell. The temperature of the solvent was varied from 0 to 80 °C and was maintained within ±0.5 °C.

Pump−probe transient absorption measurements were performed using pulses from a 1 kHz Ti:sapphire laser system as described previously.[38,42−44] The excitation pulse was the second harmonic of the laser at 400 nm. The probe pulse between 500 and 600 nm, usually at 540 nm, was produced in a noncollinear optical parametric amplifier and was delayed with respect to the pump using a 1.5 m computer-controlled delay line. The cross correlation between the 400 nm pump pulse and the visible probe pulse ranged from ca. 120 to ca. 300 fs depending on the experiment. Variable step sizes were used to scan the time delay of the probe pulse from −10 ps to 9 ns with data obtained at ca. 416 time points. When necessary, transient difference spectra were obtained for several time delays using a white-light continuum generated in a flow cell containing ethylene glycol. These data were used to confirm the assignment of the spectral features giving rise to specific decay components in the data, most importantly the geminate recombination observed following excitation of MeCbl in ethylene glycol. Most measurements were made at the magic angle to eliminate contributions due to solute reorientation. For measurement of the anisotropy decay, alternate scans were made with parallel and perpendicular polarization of the probe. UV−visible spectra taken before and after laser exposure indicated minimal sample degradation and no significant permanent photoproduct formation during the course of the typical experiments. A small buildup of aquocobalamin (H_2OCbl) was observed for some samples over the course of the experiment, but as this molecule exhibits no bond cleavage or excited state dynamics beyond ca. 10 ps the photoproduct did not interfere with measurements of geminate recombination on time scales of 100s of picoseconds to nanoseconds.

III. Results

A. Transient Absorption Data. Pump−probe transient absorption traces were obtained for methyl, ethyl, *n*-propyl, *n*-hexylnitrile, and adenosylcobalamin as a function of temperature and solvent. The data were modeled according to kinetic schemes reported in earlier papers.[42,43,45] The model used for hexylnitrile is similar to that determined for ethyl- and *n*-propylcobalamin.[38,43] The discussion below presents first the results for adenosylcobalamin followed by the results for ethyl-, *n*-propyl-, and hexylnitrile cobalamins. In each of these systems the longest decay is assigned on the basis of the transient difference spectrum to competition between geminate recombination and diffusive cage escape. The traces obtained in methylcobalamin are presented in the final section. These data

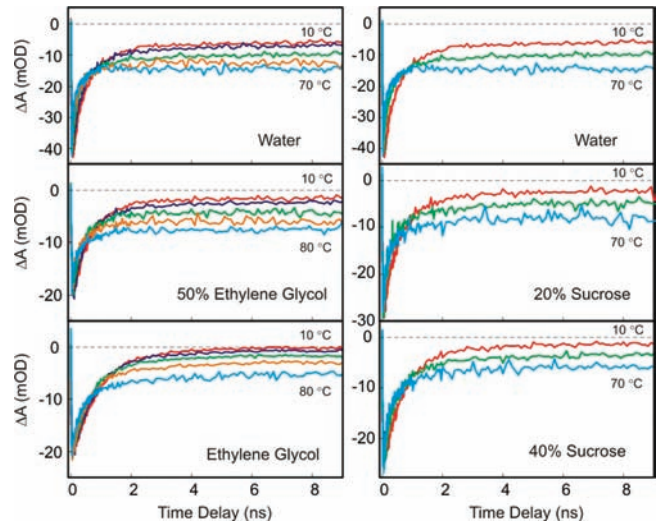

Figure 3. Transient kinetic traces following excitation of adenosylcobalamin at 400 nm. The probe wavelength was 520 nm in water and ethylene glycol and 540 nm in the 50/50 mixture of water and ethylene glycol and in sucrose solutions. The approximate temperatures are 10 °C (red), 20 °C (dark blue), 40 °C (green), 60 °C (orange), and 70 or 80 °C (light blue) as indicated.

are complicated by branching between prompt dissociation (30−40%) and formation of a long-lived excited state.[39,41,45] The kinetic model and analysis described for methylcobalamin are described below in greater detail.

i. Adenosylcobalamin. Pump−probe transient absorption traces were obtained for adenosylcobalamin in water, ethylene glycol, mixtures of water and ethylene glycol (75:25, 50:50, and 25:75 by volume), and 20% and 40% sucrose solutions for temperatures between 0 and 80 °C. The temperature limits in each case were determined by the properties of the specific solution. Typical data are plotted in Figure 3. These data demonstrate the dependence of the apparent recombination rate and the magnitude of the net cage escape on temperature and sample viscosity. In ethylene glycol at 10 °C the primary geminate recombination is nearly complete with only 1−2% of the initial radical pairs surviving to form solvent separated radical pairs. On the other extreme the yield of solvent separated radical pairs approached 60% in water at 70 °C and 40% in ethylene glycol at 80 °C.

The data were fit as described previously to a model consisting of a sum of exponentials.[38,40,42] With water present in the solution, there is a decay component that corresponds to a decrease in the magnitude of the bleach as the radical pair is produced. This component is not present in ethylene glycol. Thus four exponential components were included for the samples in neat ethylene glycol and five exponential components in all of the rest of the samples (a more detailed discussion of the model is presented in ref. 42). The longest decay component represents the sum of the escape and recombination rates. The quantum yield for production of the long-lived radical pair state was calculated as described previously.[42] A table summarizing the data is included in Supporting Information. The rate constant for recombination is scattered, but generally shows no significant dependence on temperature or solvent viscosity. The average rate constant for recombination is 1.07 ± 0.25 ns^{-1}. The rate constant for cage escape ranges from 0.016 to 2.06 ns^{-1} and the quantum yield for formation of long-lived radical pairs ranges from 1.5% to 67%. These quantities are strongly dependent on both temperature and solvent viscosity.

ii. Ethyl-, Propyl-, and Hexylnitrilecobalamins. In order to test the dependence of cage escape on the nature of the alkyl

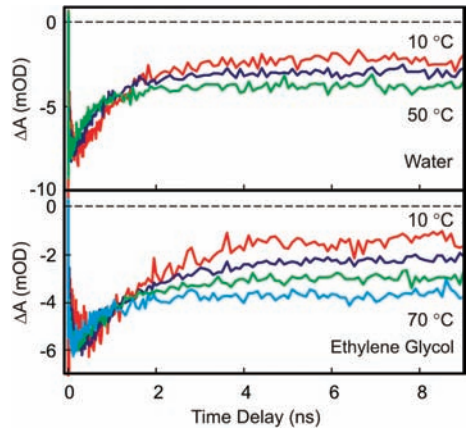

Figure 4. Transient kinetic traces following excitation of *n*-hexylnitrilecobalamin at 400 nm. The probe wavelength was 540 nm. The approximate temperatures are 10 °C (red), 30 °C (dark blue), 50 °C (green), and 70 °C (light blue). Data were also obtained for a 50:50 mixture of ethylene glycol and water by volume.

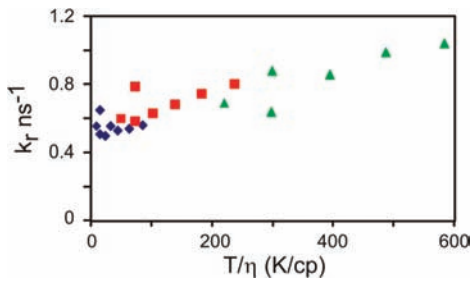

Figure 5. Recombination rate constant for hexylnitrilecobalamin as a function of solvent fluidity. The blue diamonds are in ethylene glycol, the red squares are in a 50/50 mixture of ethylene glycol and water, and the green triangles are in water.

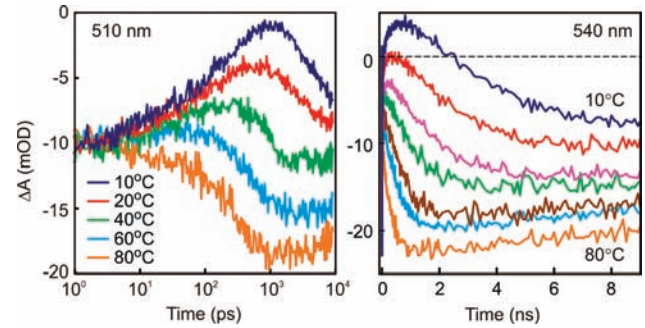

Figure 6. Transient kinetic traces obtained following excitation of methylcobalamin in ethylene glycol at 400 nm. The approximate temperatures are indicated in the left panel. For the 540 nm probe plotted in the right panel, additional traces were obtained at 30 °C (magenta) and 50 °C (brown). The traces obtained at 510 nm on the left are plotted on a logarithmic time scale to emphasize the recombination component. The traces obtained at 540 nm on the right are plotted on a linear time scale to emphasize the S_1 state decay.

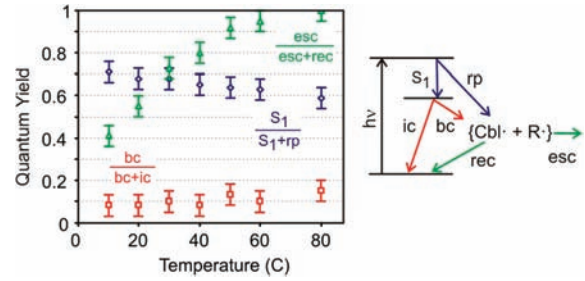

Figure 7. Quantum yields as a function of temperature for internal conversion to S_1 (blue diamonds), bond cleavage from S_1 (red circles), and geminate recombination of methylcobalamin (green triangles) in ethylene glycol following excitation at 400 nm.

radical, data were also obtained for ethyl, *n*-propyl, and *n*-hexylnitrile cobalamins. Sample traces for HxnCbl in water and ethylene glycol are shown in Figure 4. Data were obtained for temperatures of approximately 10, 20, 30, 40, and 50 °C in water, ethylene glycol, and a 50/50 mixture by volume of water and ethylene glycol. Data were also obtained at 60 °C in the latter two solvents and at 70 °C in ethylene glycol. The formation of the radical pair on a time scale of ca. 100 ps is followed by cage escape or formation of a solvent-separated radical pair. Similar traces were obtained for ethyl and *n*-propylcobalamins.

The kinetic traces were fit to a model consisting of a biexponential rise of the radical pair signal and an exponential decay representing the competition between cage escape and primary geminate recombination. This model was developed in earlier studies of ethylcobalamin and *n*-propylcobalamin.[38,43] A table summarizing the data for cage escape and primary geminate recombination following excitation of EtCbl, PrCbl, and HxnCbl is included in Supporting Information. As for adenosylcobalamin, the rate constant for recombination for EtCbl and PrCbl is scattered but shows no significant dependence on temperature or solvent viscosity. HxnCbl, however, exhibits a clear increase in the rate constant as a function of solvent fluidity (Figure 5). The average rate constant for recombination is 0.89 ± 0.19 ns^{-1} for PrCbl and 0.81 ± 0.33 ns^{-1} for EtCbl. The recombination is slower for all of the alkyl radicals than for the adenosyl radical but does not seem to depend much on the specific radical investigated. The rate constant for cage escape ranges from 0.12 to 0.99 ns^{-1} for hexylnitrile radical, 0.13 to 1.8 ns^{-1} for *n*-propyl radical, and 0.24 to 2.8 ns^{-1} for ethyl radical. The quantum yields for formation of long-lived radical pairs are strongly dependent on both temperature and solvent viscosity.

iii. Methylcobalamin. Finally, measurements were made for methylcobalamin in ethylene glycol, in mixtures of water and ethylene glycol, and in sucrose solutions. Although a geminate recombination component is not evident in water except at 10 °C, a recombination component is evident in the more viscous solvents. Data obtained in ethylene glycol with 510 and 540 nm probe wavelengths are plotted in Figure 6. Data were also obtained using 520 and 600 nm probe wavelengths. In addition, difference spectra were measured at 10, 40, and 80 °C and time delays ranging from 20 ps to 8 ns to confirm the model used in the analysis of the data. The rising component at early times (<1 ns) correlates with the disappearance of a cob(II)alamin difference spectrum leaving a pronounced contribution from the S_1 excited state absorption. The S_1 absorption spectrum decays on a nanosecond time scale leaving a small yield for the production of solvent separated radical pairs.

The data obtained following 400 nm excitation were analyzed using the model developed earlier (see Figure 7).[41,45] Excitation results in rapid formation of a radical pair or rapid internal conversion to the S_1 state. The S_1 state decays on a nanosecond time scale at room temperature to form a radical pair with small yield (ca. 15% in water). The remaining molecules return to the MeCbl ground state. These branching ratios may be temperature dependent. In ethylene glycol the contribution to the signal arising from geminate recombination of the prompt radical pair is temperature dependent. The data were analyzed using this model to extract the rate constant for geminate recombination and cage escape (Figure 7). The quantum yield

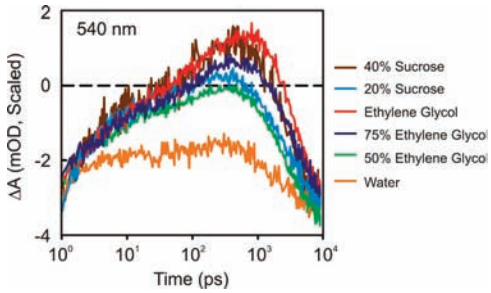

Figure 8. Transient kinetic traces for methylcobalamin following excitation at 400 nm. The temperatures are 6.8 °C in 20% Sucrose, 8.2 °C in 40% sucrose, 8.5 °C in 75% ethylene glycol, 8.4 °C in 50% ethylene glycol, and 10 °C in both ethylene glycol and water.

for cage escape is 0.4 at 10 °C and increases to unity at the highest temperatures. The quantum yield for production of the S_1 state is slightly temperature dependent. The small temperature dependence observed for the branching between internal conversion (ic) and bond cleavage (bc) from the S_1 state likely reflects the geminate recombination of the radical pair.

Transient kinetic traces at 540 nm were also obtained in a range of solvent mixtures as a function of temperature. Data obtained near 8 °C are summarized in Figure 8. These data exhibit the same recombination component observed in ethylene glycol with somewhat different escape rates and yields for geminate recombination.

The transient data are summarized in a table included in Supporting Information. The average recombination rate constant for MeCbl is 1.9 ± 0.5 ns^{-1} with no obvious temperature or solvent dependence, although the uncertainties are rather large and the temperature range small for most solvents. The temperature range surveyed was limited by the ability to extract the recombination component from the other components of the signal. This requires good signal-to-noise and a reasonable quantum yield for recombination. The rate constant for cage escape ranged from 1.3 to 23 ns^{-1}, strongly dependent on solvent and temperature.

B. Cage Escape. The standard place to start when investigating the influence of solvent on diffusive cage escape is with the Stokes−Einstein expression for the diffusion coefficient. In the simple hydrodynamic model, the rate constant for cage escape is proportional to the translational diffusion coefficient of the solute radical in the solvent. The diffusion coefficient is related to radical radius and solvent viscosity by the formula in eq 1 above for spherical radicals. For a spherical particle in a solvent of comparable or larger size, where approximation of the solvent as a "hydrodynamic continuum" is not appropriate, the factor of 6π in the denominator of eq 1 is replaced by $\alpha\pi$, where α is a variable factor determined by the effective path length taken by the solvent to exchange places with the solute. This expression may also be generalized to describe the diffusion of ellipsoidal molecules. These considerations suggest that plots of the rate constant for escape versus solvent fluidity (T/η) will provide a useful means to characterize the escape process.

While there is considerable tabulated viscosity information available for pure water and pure ethylene glycol, there is far less data available for mixtures of water and ethylene glycol. Fortunately, at least two groups have studied the viscosity properties of, and provided fits for, these mixtures over a sufficiently wide range of concentration variations and temperatures, so as to cover all compositions and temperatures needed to analyze the data presented here.[46,47] The numbers from Teja and co-workers are used in what follows and reported in the tables.

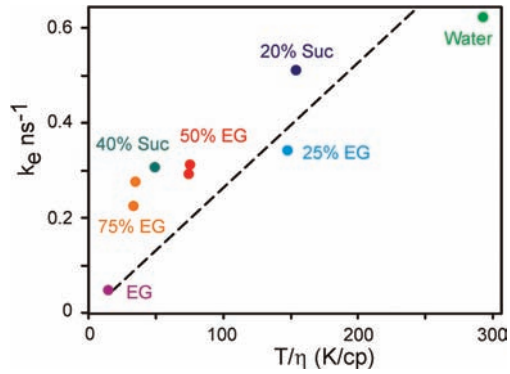

Figure 9. Data obtained for cage recombination of adenosylcobalamin at 19.9−20.7 °C in a variety of solvents. The correlation is slightly better for data obtained at 8−10 °C and worse for the data at 39−41 or 59−62 °C (not shown).

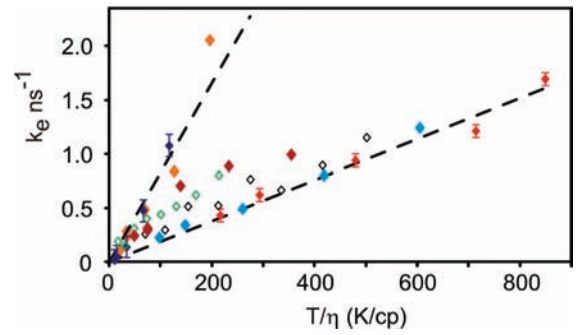

Figure 10. Rate constant for cage escape of the adenosyl radical as a function of solvent fluidity in water (red with error bars), 25% ethylene glycol (light blue), 50% ethylene glycol (maroon), 75% ethylene glycol (orange), ethylene glycol (dark blue with error bars), 20% sucrose (open black diamonds), and 40% sucrose (open green diamonds). The dashed lines are linear fits to the data in ethylene glycol and water.

There is a considerable literature on to the viscosity of solutions made from sucrose dissolved in water. Sucrose solutions are important as a gradient medium for the separation of biological material in centrifuges, requiring viscosity information as a function of temperature and sucrose concentration. In what follows we use the fits of Barber to calculate the viscosity at the desired temperature.[48,49]

i. Adenosylcobalamin. It is common in much of the literature to explore the influence of solvent on cage escape and geminate recombination by varying the solvent or solvent composition at a constant temperature. If the data for adenosylcobalamin obtained at temperatures between 19.9 and 20.7 °C is plotted as a function of fluidity, there is a correlation between k_e and $1/\eta$ but the correlation is weak and the scatter significant (Figure 9). Similar trends are observed for other temperatures.

The apparent trend in Figure 9 is misleading though. The dependence on fluidity at a given temperature is distorted by a much more significant dependence on the nature of the solvent. The rate constant for cage escape is plotted as a function of solvent fluidity in Figure 10 for photolysis of AdoCbl over the entire temperature range investigated. Clearly the data do not follow eqs 1 and 2 in any simple fashion. In any given solvent the data are reasonably well approximated by a straight line, but the slope depends on the solvent, with a much steeper slope in ethylene glycol than in water. The data in 75% ethylene glycol follow essentially the same line as that in 100% ethylene glycol. Likewise the data in 75% water solution (25% ethylene glycol) follow essentially the same line as that in 100% water. The data in the 50/50 solvent mixture fall between the two extremes. The data in 20% sucrose solution fall slightly above the line

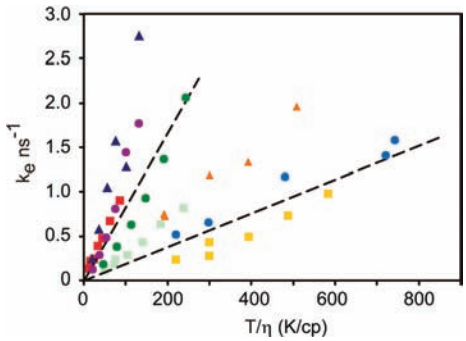

Figure 11. Rate constant for cage escape of the alkyl radicals as a function of solvent fluidity. The squares are for the hexylnitrile radical in water (yellow), 50% ethylene glycol (light green), and ethylene glycol (red). The circles are for the propyl radical in water (light blue), 50% ethylene glycol (dark green), and 75% ethylene glycol (purple). The triangles are for the ethyl radical in water (orange) and ethylene glycol (dark blue). The dashed lines are for adenosylcobalamin in water and ethylene glycol as plotted in Figure 10.

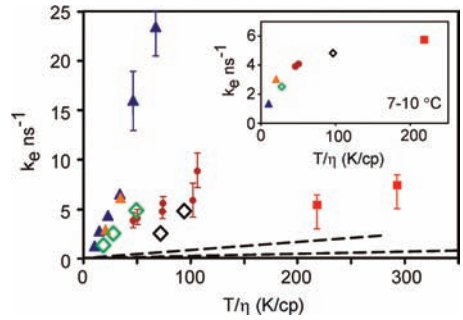

Figure 12. Rate constant for cage escape of the methyl radical as a function of solvent fluidity in water (red squares), 50% ethylene glycol (maroon circles), 75% ethylene glycol (orange triangles), ethylene glycol (dark blue triangles), 20% sucrose (open black diamonds), and 40% sucrose (open green diamonds). The dashed lines are for adenosylcobalamin in water and ethylene glycol as plotted in Figure 10. The insert highlights the behavior as a function of solvent at approximately constant temperature.

for 100% water, while the data in 40% sucrose solution fall between the extremes.

ii. Ethyl-, Propyl-, and Hexylnitrilecobalamin. The adenosyl radical is large, rigid, and has several NH and OH groups capable of specific interaction with the water and ethylene glycol solvents used in these experiments. The influence of radical on the diffusive cage escape was explored by expanding the study to include ethyl, propyl, and hexylnitrile radicals. The first two represent examples of small nonpolar radicals, while hexylnitrile is somewhat larger and flexible. The rate constants for cage escape as a function of solvent fluidity are plotted in Figure 11. The data follow the same trends observed for the adenosyl radical. The rate constants for the escape of the hexylnitrile and propyl radicals in water fall near the line observed for adenosyl in water with hexylnitrile slightly lower and propyl radical slightly higher than adenosyl. The rate constant for escape of the ethyl radical is substantially faster than those for the larger radicals. The rate constants for cage escape in 75% ethylene glycol (ethyl and propyl) or 100% ethylene glycol (hexylnitrile) fall above the line observed for adenosyl radical in 100% or 75% ethylene glycol solutions. The data in 50/50 solvent mixtures for propyl and hexylnitrile radicals fall between the two extremes.

iii. Methylcobalamin. The rate constant for the diffusive escape of the methyl radical is much larger than that for any of the other radicals studied. These data are plotted as a function of solvent fluidity in Figure 12. The trends are similar to those observed for the larger radicals. The accessible range of fluidity is much smaller for the methyl radical as the quantum yield for cage escape quickly approaches unity as the temperature increases. The numbers reported for water are estimates from a very small amplitude decay component observed at the lowest temperatures only. The large error bars on these two data points and for the two highest temperature points in ethylene glycol arise from the difficulty of determining an accurate quantum yield for escape at these temperatures and intrinsic errors in the decay constant for this small amplitude component. For the two data points in water and these two data points in ethylene glycol, the quantum yield for cage escape is greater than 90%. The error bars are also indicated for data obtained in the 50/50 mixture of water and ethylene glycol. For the remainder of the data, the error bars are comparable to the size of the markers.

IV. Discussion

The qualitative discussion above can be placed on a more quantitative footing. In this experiment we produce radical pairs at or near thermal equilibrium with the surrounding and watch the decay of this radical population. The decay of the primary geminate pair in most of the measurements reported here is well approximated by a single exponential decay to a plateau. Some of the data at the highest temperatures begin to show evidence of a nonexponential or mutiexponential decay and some secondary geminate recombination of radical pairs following the initial cage escape process. The numbers reported however are dominated by the "unimolecular" decay of a radical pair surrounded by solvent molecules. With no specific interaction between the neutral radicals the lifetime of the contact pair is determined by the molecular diffusion. Thus we suggest that this decay will occur at approximately the steady state rate in the initial analysis.

A. Influence of Radical Reorientation on Recombination. Both diffusive cage escape and diffusive reorientation of the cob(II)alamin and the alkyl radicals are expected to correlate with the solvent fluidity with the reorientation time given by $\tau_R \propto \eta/T$. This may be important as the radical recombination requires a compatible orientation for the two radicals. Thus the dependence of the observed escape rate on fluidity may be a function of both translational and rotational diffusion. The reorientation time for the cob(II)alamin radical may be determined from the anisotropy decay of the signal following excitation of any of the alkylcobalamins. Such a measurement following excitation of adenosylcobalamin at 20 °C in water yielded a reorientation time of 1.41 ± 0.05 ns for the cob(II)alamin radical. This time constant is consistent with the size and shape of the radical and the fluidity of the solution. Most of the experiments were conducted at lower fluidity and the reorientation time will be slower. In every case the reorientation is significantly slower than the recombination and cobalamin reorientation should play little role in the geminate recombination process.

We have no direct probe to measure the reorientation of the alkyl radicals. Experimental measurements on small molecules, similar in size and shape to the radicals investigated here, permit estimates of the room temperature reorientation. The reorientation time of ammonium, a spherical cation slightly smaller than the methyl radical, ranges from 0.93 ps in water to 12.4 ps in ethylene glycol,[50] a range qualitatively consistent with the anticipated dependence on viscosity. The reorientation time of

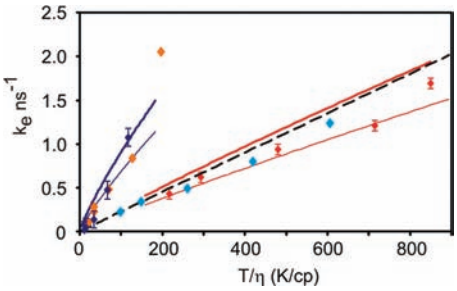

Figure 13. Calculations of cage escape for adenosylcobalamin. Diamonds are data obtained in water (red), 75% water (lt blue), 75% ethylene glycol (orange), and ethylene glycol (blue). The black dashed line is a Stokes−Einstein calculation using eqs 1 and 2. The lines are calculations using eq 4a assuming both radicals diffuse (thick lines) or only the adenosyl radical diffuses (thin lines).

molecules comparable in size to the Ado radical are on the order of 70−140 ps/(mPa s) at room temperature.[50−58] Reorientation of the Et and Pr radicals will be slower than anticipated for Me but much faster than the reorientation of the Ado radical. Thus, reorientation of the small alkyl radicals is anticipated to be rapid with respect to the observed recombination rate, while reorientation of the Ado radical will be on a time scale comparable with (water) or slower than (ethylene glycol) the recombination at room temperature. There is no apparent correlation between recombination rate and solvent fluidity for methyl, ethyl, propyl, or adenosylcobalamin supporting the conclusion that recombination rate for the smaller radicals reflects an orientational average while the recombination rate for the adenosyl radical is not substantially influenced by reorientation. Hexylnitrile is an exception to the above analysis with a distinct correlation between solvent fluidity and recombination. The hexylnitrile radical is larger and/or more flexible than the other radicals and it is likely that reorientational and conformational dynamics of the radical result in an effective recombination rate which depends on solvent fluidity.

B. Hydrodynamic Stokes−Einstein Diffusion. In a hydrodynamic model the escape rate is equated to the dissociation rate and plotted versus the fluidity for a quantitative comparison. For adenosyl radical in solution the radius r can be estimated as 4.1 Å (based on measurements of the molar volume of adenosine).[59,60] The radius used for adenosyl is slightly larger than the 3.8 Å radius estimated from the calculated van der Waals volume,[43] which may be important when we consider the other alkyl radicals below. The estimate for adenosyl is slightly smaller than the 4.42 Å radius obtained in the diffusion measurements of adenosine.[61] The radius of the cobalamin radical is estimated at 7.1 Å based on measurements of the partial molar volume of simple cobalamins.[62] This is consistent with the radius estimated from the calculated molar volume using the LeBas correction.[63] The hydrodynamic radius of vitamin B_{12} has also been estimated at 8.5 Å from diffusion measurements assuming a spherical molecule,[64,65] thus 7.1 Å should be considered a lower limit. The reactive radius is taken to be the sum of these $R = 11.2$ Å. The rate constant $k_e(T/\eta)$ calculated using eq 2, assuming the Stokes−Einstein model for diffusivity (eq 1), $D = D_{Alkyl} + D_{Cob}$, and $R = 11.2$ Å, is in reasonable quantitative agreement with the observation in water (Figure 13). But the simple Stokes−Einstein hydrodynamic model provides no explanation for the variation in the slopes in different solvents.

C. Solvent-Dependent Corrections to the Diffusion Coefficient. Diffusion has been heavily studied and many more sophisticated and potentially more accurate models for diffusivity have been explored. Multiple expressions for the diffusion coefficient are in common use, but these are often limited in terms of environmental application, involve unknown empirical parameters, or are limited to self-diffusion. The Stokes−Einstein expression for the diffusion coefficient assumes that a large particle is diffusing in a solvent composed of much smaller molecules. The Eyring expression is one of the earliest theories designed to take into explicit account the relative sizes of the solvent and solute molecules.[66,67] In the limit that the diffusing particle and the solvent are the same size the diffusion coefficient is given by

$$D = \frac{k_b T}{\eta}\frac{\lambda_a}{\lambda_b \lambda_c} \tag{3}$$

where λ_a is the perpendicular distance between two neighboring layers of molecules—generally less than $2r$ where r is the molecular radius, λ_b is the distance between neighboring molecules in the direction of motion, and λ_c is the molecule to molecule distance in the plane normal to the direction of motion.

Akgerman and Gainer proposed and characterized a model for diffusivity of molecules of differing size that is an extension of the Eyring model using molar volumes to account for the relative sizes and displacements of the solvent and solute.[68] The Akgerman model uses the following expression for diffusion constants

$$D = \frac{k_b T}{\xi \eta}\left(\frac{N}{V_{solv}}\right)^{1/3}\left(\frac{M_{solu}}{M_{solv}}\right)^{1/2} \exp\left(\frac{E_\eta - E_D}{RT}\right) \tag{4a}$$

$$\xi = 6\left(\frac{V_{solu}}{V_{solv}}\right)^{1/6} \tag{4b}$$

V is the molar volume of the solute/solvent, M the molar mass, k_b is the Boltzmann constant, R the gas constant, and N Avogadro's number. ξ is a parameter that accounts for the number of solvent molecules surrounding the solute molecule. E_η is the activation energy for viscosity, and E_D the activation energy for diffusion. The Agkerman-Gainer model considers explicitly the relative probability that either a solute or solvent molecule will be in the transition state to fill a hole which has opened in its vicinity. The factor (M_{solu}/M_{solv}) in eq 4a arises from the ratio of the transition state partition functions. This model provides an approach to begin to explain and interpret the solvent and radical differences observed in the present study.

To apply this model to calculate the diffusion coefficients for the alkyl radicals studied here, we need estimates for the molar volumes of the solvents and solutes and estimates for the activation energies. Akgerman and Gainer used LeBas values to calculate the molar volumes.[68,69] We have used estimates based on measurements of the molar volume for water, ethylene glycol, adenosyl, and the cobalt ring structure. For the other alkyl radicals, the molar volume was determined from the van der Waals volume calculated with Spartan. The van der Waals volume can be related to the LeBas volume as $V_{LB} = 1.15V_{vdW}$.[63] This choice of parameters results in close agreement with the diffusivities tabulated by Akgerman,[69,70] for those solutes where comparison is possible. The method for calculating the difference in activation energies is based on the energy necessary for a solvent or solute molecule to occupy a hole in the solvent, which may be significant in associated solvents where hydrogen

bonds must be broken before obtaining the activated state for flow.[68−70] Akgerman and Gainer proposed the following expression to calculate the difference

$$E_\eta - E_D = E_{BB} - E_{AB} \quad (5)$$

E_{AB} and E_{BB} are the jumping activation energies required for a solute molecule to fill a hole and a solvent molecule to fill a hole, respectively. E_{BB} is calculated by Akgerman and Gainer for a range of solvents according to the method of Glasstone et al.[71] from solvent viscosity and found to be 4.3 kcal/mol for water and 7.1 kcal/mol for ethylene glycol over the range of 0−70 °C. E_{AB} was estimated based on the probability of the "jumping" to fill a hole as

$$E_{AB} = E_{BB}^{\xi/\xi+1} E_{AA}^{1/\xi+1} \quad (6)$$

Akgerman has tabulated E_{AA} in expression 6 by correlating the experimental data with molecular weight.

$$E_{AA} = 5875.3 M_{solu}^{-0.186} \quad (7)$$

where the molar mass is given in g/mol and E_{AA} in cal/mol.

This model for diffusivity represents a significant improvement in explaining the gross features of the data. Indeed, the agreement with adenosylcobalamin data is excellent as shown in Figure 13. The model accounts very well for the relative escape rates in ethylene glycol and water solutions. Because the estimate for the diffusion coefficient of the cob(II)alamin radical may overestimate the mobility of this radical, especially as the radical interacts strongly with the solvent, we have calculated the rate constant for cage escape assuming $D_{Cob} \approx 0$ and D_{Cob} calculated as described above—i.e., both radicals diffuse, or only the alkyl radical diffuses. The agreement is nearly quantitative, with the data falling between the two limiting rates.

The dominant factor contributing to the observed solvent dependence is the factor $(M_{solu}/M_{solv})^{1/2}$ arising from the ratio of the transition state partition functions. Turning attention to the influence of radical size on cage escape, the model does not fare quite as well. When parameters appropriate for the hexylnitrile, propyl, or ethyl radicals are used and the data are compared with the experimental cage escape rates, the model overestimates the escape rate by a factor of 2 or 3 but reproduces the solvent dependence. The predicted and measured rate constants in water are plotted in Figure 14 for all three radicals. The model predicts a substantial increase in the escape rate for all three radicals while the data show a slight decrease for the hexylnitrile radical, slight increase for the propyl radical, and a somewhat larger increase for the ethyl radical.

The model still provides a qualitative explanation for the solvent dependence. A multiplicative factor of 0.46 for hexylnitrile radical, 0.44 for ethyl radical, and 0.32 for propyl radical yields qualitative agreement with the data in both solvents (see Figure 15). Likewise, the model reproduces the solvent trend for methyl radical with a multiplicative factor of 3.3 ± 0.1. For methyl, ethyl, and propyl radicals the same constant accounts for both solvents. For hexylnitrile the constant is an average the best fits in the two solvents (0.36 in water and 0.55 in ethylene glycol).

The need for a multiplicative factor is interesting. If the expression derived by Akgerman and Gainer accurately accounts

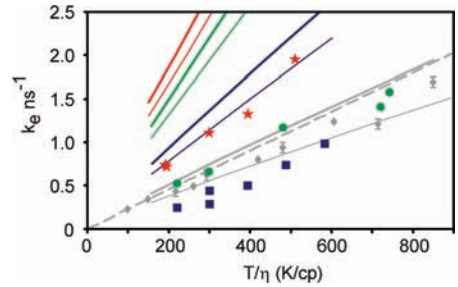

Figure 14. Comparison of calculated and experimental cage escape for adenosyl, propyl, and hexylnitrile radicals in water. The gray lines and symbols are the data for adenosyl radical as plotted in Figure 13. The blue squares are the data for hexylnitrile, the green circles are the data for propyl, and the red stars are the data for ethyl. The solid lines are calculations using eq 4b assuming both radicals diffuse (thick lines) or only the alkyl radical diffuses (thin lines).

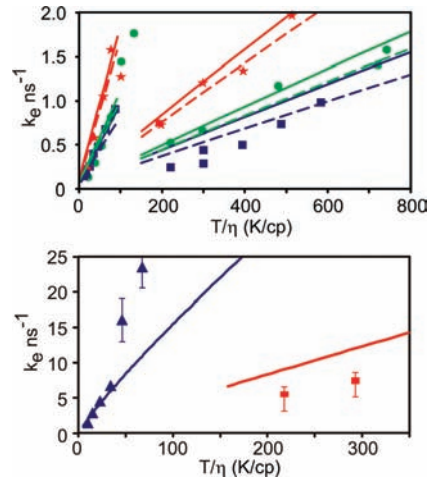

Figure 15. Top: Escape rates for hexylnitrile (blue squares) and propyl (green circles) and ethyl (red stars) in ethylene glycol and water. The lines are the calculations using eqs 2 and 3 for diffusion of both radicals (solid) or just the alky radical (dashed) with multiplicative factors of 0.46, 0.32, and 0.44, respectively. Bottom: Escape rates for methyl in water (red) and ethylene glycol (blue). The lines are the calculations for methyl diffusion with a scale factor of 3.3.

for the diffusivity of the radical through the solvent, this scale factor likely arises at least in part from an underestimate of the effective hydrodynamic radius. If the entire effect is attributed to radical size, the data suggest that the effective radical sizes are roughly twice that predicted from the van der Waals radii. For the ethyl radical the effective radius is estimated at ca. 4.5 Å compared with the estimate of 2.3 Å obtained from the calculated van der Waals volume. The effective radius for the propyl radical is approximately 6.1 Å compared with the calculated estimate of 2.5 Å. The effective radius for the hexylnitrile radical is approximately 4.7 Å in ethylene glycol and 6.4 Å in water compared with the calculated estimate of 3.1 Å. The difference in the effective radius may arise from the shape and conformational flexibility of these small alkane chains. Alternatively factors other than effective radius may contribute to the observed discrepancy in the quantitative prediction of escape rates.

The analysis above has not explicitly considered the geminate recombination in the solvent mixtures. The data in 75% ethylene glycol mixtures follow the line calculated for ethylene glycol, while the data in 25% ethylene glycol follow the line calculated for water solvent. These observations suggest that the influence of solvent molar mass and volume on the diffusion coefficient is dominated by the major component of the solvent. The behavior of both methyl and adenosyl in the 20% sucrose

mixture is only slightly different than those in 100% water or 25% ethylene glycol suggesting that displacement of water again plays a major role in the diffusive cage escape. The 40% sucrose mixtures and the 50/50 mixtures of water and ethylene glycol are more interesting. In these systems the rate constant for cage escape falls near the mean of the data in ethylene glycol and water suggesting that the influence of solvent parameters on the diffusion constant is in effect a weighted average of the two components.

D. Other Considerations. ***i. Radical Proximity.*** An important assumption made above is that the total diffusivity is the simple sum of the steady-state diffusivity for each radical. However, for the case of relative diffusion of two molecules in close proximity to each other, it is known that the overall diffusive coefficient is reduced due to coordination between the molecules. The diffusion of each molecule is hindered by the presence of the other resulting in a spatially dependent diffusivity. Certainly the diffusion of the smaller alkyl radical will be hindered by the presence of the large cobalamin in close proximity. The smaller diffusivity will result in a smaller rate constant for the dissociation of radical pairs, in agreement with the observed trends. Thus it is also possible that this effect accounts for some of the deviation between the calculated and experimental escape rates for the alkylcobalamins. Hynes has offered eq 8 as a reasonable empirical approximation.[72]

$$D(r) = D_0\left(1 - \frac{1}{2}e^{-(r-R)/R}\right) \tag{8}$$

The qualitative influence of eq 8 on the escape rate is consistent with the observations for hexylnitrile and propylcobalamin. In the initial cage escape process it is reasonable to assume that $r \approx R$. In this limit eq 8 reduces to $D(r) = D_0(1 - 0.5) = 0.5D_0$. This factor of 0.5 is of the same order as the observed factors of 0.34−0.5. However, this effect does not account for the behavior of the methyl radical where the cage escape is much faster than that predicted.

ii. The Methyl Radical. The cage escape of the methyl radical is substantially faster than that predicted by simple hydrodynamic models. It is possible that the size of the methyl radical facilitates a faster cage escape, although radical size does not account for the fast cage escape observed in other systems where the radicals are much larger.[29,32] In this regard it is important to note that the photodissociation of methylcobalamin produces the radical pair through excitation to a directly dissociative state.[38,39,41,43] The momentum imparted in the photoexcitation can have a substantial impact on the cage escape and geminate recombination.[73] For all of the other systems studied the radical pair is produced following internal conversion to a lower excited state, often with a substantial delay between excitation and the formation of the radical pair. Thus the radical pairs are produced in thermal equilibrium with the surroundings. Direct photodissociation, as for methyl radical here, may accelerate the cage escape by producing radical pairs with excess kinetic energy in the recoil.

iii. More Sophisticated Models. In this paper we have analyzed a substantial data set in the context of a rather simple hydrodynamic model using one parameter—an exponential rate constant for cage escape. The model accounts for the gross features of the data quite well, including the dependence of this escape rate on viscosity, solvent, and temperature. Moving beyond hydrodynamic and rate theory models for cage escape, one may apply a kinetic theory for the geminate recombination of photoinduced caged radical pairs calculating the pair survival rate as a function of time[8,72,74−80] A kinetic model based on a generalized Langevin approach has been formulated to calculate the survival probability of the radical pair as a function of time, still with the assumption of hard spheres for both solute and solvent molecules. In the long time limit, the kinetic model reproduces the hydrodynamic results of Collins and Kimball.[36,37] Several groups have used this time-dependent result to analyze photolysis data, by fitting directly the time-dependent expression for the probability of pair survival (convoluted with an appropriate instrument response function) to the transient data, where the fitting parameters are (1) the ratio of the initial separation, r_0, to the reaction radius, R, (2) the ratio of the bimolecular rates for recombination and diffusion, and (3) the ratio of the elapsed time to the diffusive time constant, R^2/D ($=1/k_e$, above).[20,21,32] Such fits, however, still require an estimate for the diffusivity, D, to provide physically relevant parameters.

One serious limitation of both hydrodynamic and kinetic models of diffusion is the assumption of hard spheres or even ellipsoids for solvent and solute. Both the propyl and the hexylnitrile radicals have a capacity for conformational fluctuation likely to complicate the diffusion process. The most promising approach to analyze the cage escape appears to come from atomistic molecular dynamics simulations. Such simulations should be able to capture the radical specific dynamics and account for the contrast in behavior of ethyl, propyl, and hexylnitrile radicals in water and ethylene glycol.

V. Conclusions

In this paper we have explored the geminate recombination of cob(II)alamin with several alkyl radicals as a function of temperature and solvent composition. These results demonstrate that geminate recombination of contact radical pairs occurs on time scales ranging from a few tens of picoseconds for methyl radical at high fluidity to more than a nanosecond for the larger radicals at low fluidity. These time scales are much slower than those expected based on earlier work on recombination following direct photodissociation, where the time scale for cage escape is typically picoseconds. The time scales reported here are, however, in excellent agreement with the predictions based on hydrodynamics theories and experimentally determined steady-state diffusion constants for all of the radicals except the methyl radical. The near quantitative agreement between the observed data for adenosylcobalamin and the escape rates calculated by using the formula derived by Agkermann and Gainer for the diffusion coefficients illustrates that the hydrodynamic model accounts for the general features of the process. The cage escape process is well modeled as a unimolecular activated process characterized by an exponential decay. For any given solvent or solvent mixture the escape rate depends approximately linearly on the solvent fluidity. However comparisons of radical recombination at constant temperature, changing the fluidity by using solvents of different viscosity, are problematic. These plots should not be expected to agree with simple theories as the dependence of k_e on fluidity is convoluted with the dependence on solvent mass and volume.

These results and the extensive data set presented above should stimulate further experimental and theoretical studies of influence of local environment on primary geminate recombination of reactive species in solution.

Acknowledgment. This work was supported by grants from the National Science Foundation CHE-0718219 and CHE-0078972. XD, BS, and JW were supported by summer 2008 REU programs at Michigan. The authors also acknowledge Professor Ken Spears for helpful discussion and advice.

Supporting Information Available: Tables summarizing the cage escape and geminate recombination as a function of temperature and solvent for adenosyl, methyl, ethyl, *n*-propyl, and hexylnitrilecobalamins. This information is available free of charge via the Internet at http://pubs.acs.org.

References and Notes

(1) Lampe, F. W.; Noyes, R. M. *J. Am. Chem. Soc.* **1954**, *76*, 2140–2144.
(2) Noyes, R. M. *J. Chem. Phys.* **1954**, *22*, 1349–1359.
(3) Noyes, R. M. *J. Am. Chem. Soc.* **1955**, *77*, 2042–2045.
(4) Gerards, L. E. H.; Bulthuis, H.; de Bolster, M. W. G.; Balt, S. *Inorg. Chim. Acta* **1991**, *190*, 47–53.
(5) Gerards, L. E. H.; De Bolster, M. W. G.; Balt, S. *Inorg. Chim. Acta* **1992**, *192*, 287–290.
(6) Hippler, H.; Troe, J.; Luther, K *Chem. Phys. Lett.* **1972**, *16*, 174–&.
(7) Nesbitt, D. J.; Hynes, J. T. *J. Chem. Phys.* **1982**, *77*, 2130–2143.
(8) Balk, M. W.; Brooks, C. L.; Adelman, S. A. *J. Chem. Phys.* **1983**, *79*, 804–815.
(9) Kelley, D. F.; Abulhaj, N. A.; Jang, D. J. *J. Chem. Phys.* **1984**, *80*, 4105–4109.
(10) Otto, B.; Schroeder, J.; Troe, J. *J. Chem. Phys.* **1984**, *81*, 202–213.
(11) Berg, M.; Harris, A. L.; Harris, C. B. *Phys. Rev. Lett.* **1985**, *54*, 951–954.
(12) Abulhaj, N. A.; Kelley, D. F. *J. Chem. Phys.* **1986**, *84*, 1335–1344.
(13) Harris, A. L.; Berg, M.; Harris, C. B. *J. Chem. Phys.* **1986**, *84*, 788–806.
(14) Paige, M. E.; Russell, D. J.; Harris, C. B. *J. Chem. Phys.* **1986**, *85*, 3699–3700.
(15) Smith, D. E.; Harris, C. B. *J. Chem. Phys.* **1987**, *87*, 2709–2715.
(16) Philippoz, J. M.; Monot, R.; Vandenbergh, H. *J. Chem. Phys.* **1990**, *93*, 8676–8681.
(17) Xu, X. B.; Lingle, R.; Yu, S. C.; Chang, Y. J.; Hopkins, J. B. *J. Chem. Phys.* **1990**, *92*, 2106–2107.
(18) Besnard, M.; Delcampo, N.; Deviolet, P. F.; Rulliere, C. *Laser Chem.* **1991**, *11*, 109–118.
(19) Yan, Y. J.; Whitnell, R. M.; Wilson, K. R.; Zewail, A. H. *Chem. Phys. Lett.* **1992**, *193*, 402–412.
(20) Scott, T. W.; Liu, S. N. *J. Phys. Chem.* **1989**, *93*, 1393–1396.
(21) Scott, T. W.; Doubleday, C. *Chem. Phys. Lett.* **1991**, *178*, 9–18.
(22) Covert, K. J.; Askew, E. F.; Grunkemeier, J.; Koenig, T.; Tyler, D. R. *J. Am. Chem. Soc.* **1992**, *114*, 10446–10448.
(23) Lindfors, B. E.; Male, J. L.; Covert, K. J.; Tyler, D. R. *Chem. Commun.* **1997**, 1687–1688.
(24) Male, J. L.; Lindfors, B. E.; Covert, K. J.; Tyler, D. R. *J. Am. Chem. Soc.* **1998**, *120*, 13176–13186.
(25) Braden, D. A.; Parrack, E. E.; Tyler, D. R. *Coord. Chem. Rev.* **2001**, *211*, 279–294.
(26) Schutte, E.; Weakley, T. J. R.; Tyler, D. R. *J. Am. Chem. Soc.* **2003**, *125*, 10319–10326.
(27) Harris, J. D.; Oelkers, A. B.; Tyler, D. R. *J. Organomet. Chem.* **2007**, *692*, 3261–3266.
(28) Harris, J. D.; Oelkers, A. B.; Tyler, D. R. *J. Am. Chem. Soc.* **2007**, *129*, 6255–6262.
(29) Oelkers, A. B.; Scatena, L. F.; Tyler, D. R. *J. Phys. Chem. A* **2007**, *111*, 5353–5360.
(30) Oelkers, A. B.; Schutte, E. J.; Tyler, D. R. *Photochem. Photobiol. Sci.* **2008**, *7*, 228–234.
(31) Oelkers, A. B.; Tyler, D. R. *Photochem. Photobiol. Sci.* **2008**, *7*, 1386–1390.
(32) Bultmann, T.; Ernsting, N. P. *J. Phys. Chem.* **1996**, *100*, 19417–19424.
(33) Lochschmidt, A.; Eilers-König, N.; Heineking, N.; Ernsting, N. P. *J. Phys. Chem. A* **1999**, *103*, 1776–1784.
(34) Bagdasar'yan, K. S. *Russ. Chem. Rev.* **1984**, *53*, 623–639.
(35) Shin, K. J.; Kapral, R. *J. Chem. Phys.* **1978**, *69*, 3685–3696.
(36) Collins, F. C. *J. Coll. Sci.* **1950**, *5*, 499–505.
(37) Collins, F. C.; Kimball, G. E. *J. Colloid Sci.* **1949**, *4*, 422–437.
(38) Cole, A. G.; Yoder, L. M.; Shiang, J. J.; Anderson, N. A.; Walker II, L. A.; Banaszak Holl, M. M.; Sension, R. J. *J. Am. Chem. Soc.* **2002**, *124*, 434–441.
(39) Walker, L. A., II; Jarrett, J. T.; Anderson, N. A.; Pullen, S. H.; Matthews, R. G.; Sension, R. J. *J. Am. Chem. Soc.* **1998**, *120*, 3597–3603.
(40) Walker, L. A., II; Shiang, J. J.; Anderson, N. A.; Pullen, S. H.; Sension, R. J. *J. Am. Chem. Soc.* **1998**, *120*, 7286–7292.
(41) Shiang, J. J.; Walker, L. A., II; Anderson, N. A.; Cole, A. G.; Sension, R. J. *J. Phys. Chem. B* **1999**, *103*, 10532–10539.
(42) Yoder, L. M.; Cole, A. G.; Walker, L. A., II; Sension, R. J. *J. Phys. Chem. B* **2001**, *105*, 12180–12188.
(43) Sension, R. J.; Harris, D. A.; Cole, A. G. *J. Phys. Chem. B* **2005**, *109*, 21954–21962.
(44) Sension, R. J.; Harris, D. A.; Stickrath, A.; Cole, A. G.; Fox, C. C.; Marsh, E. N. G. *J. Phys. Chem. B* **2005**, *109*, 18146–18152.
(45) Harris, D. A.; Stickrath, A. B.; Carroll, E. C.; Sension, R. J. *J. Am. Chem. Soc.* **2007**, *129*, 7578–7585.
(46) Sun, T.; Teja, A. S. *J. Chem. Eng. Data* **2003**, *48*, 198–202.
(47) Bohne, D.; Fischer, S.; Obermeier, E. *Buns-Ges. Phys. Chem. Chem. Phys.* **1984**, *88*, 739–742.
(48) Barber, E. J. *NCI Monograph* **1966**, *21*, 219–239.
(49) Bouchard, C.; Grandjean, B. P. A. *Food Sci. Technol.* **1995**, *28*, 157–159.
(50) Masuda, Y. *J. Phys. Chem. A* **2001**, *105*, 2989–2996.
(51) Dutt, G. B.; Sachdeva, A. *J. Chem. Phys.* **2003**, *118*, 8307–8314.
(52) Dutt, G. B.; Raman, S. *J. Chem. Phys.* **2001**, *114*, 6702–6713.
(53) Dutt, G. B.; Krishna, G. R.; Raman, S. *J. Chem. Phys.* **2001**, *115*, 4732–4741.
(54) Dutt, G. B.; Krishna, G. R. *J. Chem. Phys.* **2000**, *112*, 4676–4682.
(55) Dutt, G. B. *J. Chem. Phys.* **2000**, *113*, 11154–11158.
(56) Dutt, G. B.; Srivatsavoy, V. J. P.; Sapre, A. V. *J. Chem. Phys.* **1999**, *111*, 9705–9710.
(57) Moog, R. S.; Ediger, M. D.; Boxer, S. G.; Fayer, M. D. *J. Phys. Chem.* **1982**, *86*, 4694–4700.
(58) Rice, S. A.; Kenney-Wallace, G. A. *Chem. Phys.* **1980**, *47*, 161–170.
(59) Dyke, B. P.; Hedwig, G. R. *J. Chem. Thermodyn.* **2008**, *40*, 957–965.
(60) Kundu, A.; Kishore, N. *J. Solution Chem.* **2002**, *31*, 477–498.
(61) Nishida, K.; Ando, Y.; Kawamura, H. *Colloid Polym. Sci.* **1983**, *261*, 1435–1536.
(62) Balt, S.; Vanherk, A. M. *Inorg. Chim. Acta* **1986**, *125*, 27–30.
(63) La-Scalea, M. A.; Souza Menezes, C. M.; Ferreira, E. I. *J. Mol. Struct.: THEOCHEM* **2005**, *730*, 111–120.
(64) Connors, T. F.; Arena, J. V.; Rusling, J. F. *J. Phys. Chem.* **1988**, *92*, 2810–2816.
(65) Peirano, F.; Vincent, T.; Guibal, E. *J. Appl. Polym. Sci.* **2007**, *107*, 3568–3578.
(66) Eyring, H. *J. Chem. Phys.* **1936**, *4*, 283–291.
(67) Hsu, C. C.; Eyring, H. *Proc. Natl. Acad. Sci.U.S.A.* **1972**, *69*, 1342–1345.
(68) Akgerman, A.; Gainer, J. L. *Ind. Eng. Chem. Fundam.* **1972**, *11*, 373–379.
(69) Akgerman, A.; Gainer, J. L. *J. Chem. Eng. Data* **1972**, *17*, 372–377.
(70) Akgerman, A. Ph.D. Dissertation University of Virginia, 1971.
(71) Glasstone, W; Laidler, K. J.; Eyring, H *Theory of Rate Processes*; McGraw-Hill: New York, 1941; pp477−551.
(72) Northrup, S. H.; Hynes, J. T. *J. Chem. Phys.* **1979**, *71*, 871–883.
(73) Koenig, T.; Scott, T. W.; Franz, J. A. *ACS Symp. Ser.* **1990**, *No. 428*, 113–132.
(74) Northrup, S. H.; Hynes, J. T. *J. Chem. Phys.* **1979**, *71*, 884–893.
(75) Cukier, R. I.; Kapral, R.; Lebenhaft, J. R.; Mehaffey, J. R. *J. Chem. Phys.* **1980**, *73*, 5244–5253.
(76) Cukier, R. I.; Kapral, R.; Mehaffey, J. R. *J. Chem. Phys.* **1981**, *74*, 2494–2504.
(77) Cukier, R. I.; Mehaffey, J. R.; Kapral, R. *J. Chem. Phys.* **1978**, *69*, 4962–4975.
(78) Ali, D. P.; Miller, W. H. *Chem. Phys. Lett.* **1984**, *105*, 501–505.
(79) Schell, M.; Kapral, R.; Cukier, R. I. *J. Chem. Phys.* **1981**, *75*, 5879–5882.
(80) Brooks, C. L.; Berkowitz, M.; Adelman, S. A. *J. Chem. Phys.* **1980**, *73*, 4353–4364.

JP9017986